Panamerican Mathematical Journal
ISSN: 1064-9735
Vol 34 No. 03 (2024)

Energy Dissipation Dynamics in Bulged Profiles in Sinter Forging

Navdeep[1,] , **Parveen Kumar** [2,] , **R. K. Ranjan** [3,]

[1, 2] Department of Mathematics, J. C. Bose University of Science and Technology, YMCA, Sector 6, Faridabad, Haryana, 121006, INDIA

[3] Department of Mechanical Engineering, Government Polytechnic, Vidya Peeth Chowk, Lakhisarai, Bihar, 811311, INDIA

Author Emails

[1] navdeepvar394@gmail.com

[2] *Corresponding author:* parveengaur1980@gmail.com

[3] rkranjanbit@gmail.com

Article History:

Received: *02-08-2024*

Revised: *15 -09- 2024*

Accepted: *24-09-2024*

Abstract: This paper explores various aspects of bulging in high-speed sinter-forging across different relative densities. The forging process of sintered preforms involves significant energy dissipation, affected by factors like die speed, bulging coefficient, initial relative density, and height reduction. High die speed results in increased frictional energy dissipation, leading to surface heating and bulging. Moreover, there is a notable increase in energy dissipation, die load, and frictional energy with a reduction in height, primarily dissipating heat on the preform surface. Total energy dissipation, die load, and frictional energy notably increase with die speed, particularly with higher bulging coefficients and initial relative densities. Additionally, inertial energy dissipation rises rapidly under these conditions. The intricate relationship between fractional internal energy dissipation and fractional frictional energy dissipation to total energy dissipation highlights the complexity of the process, with internal energy dissipation decreasing while the frictional energy dissipation component increases with bulging coefficient and relative density. At high die velocities, most energy dissipates as frictional heat, underscoring the need to control forging velocity for desired product outcomes.

Keywords*:* Sinter forging, Upper bound, bulging, dynamical effect, die load.

1. INTRODUCTION

Sinter forging combines the benefits of powder metallurgy and conventional forging to mass-produce precise engineering components with minimal scrap loss and competitive costs. It ensures robust metallurgical structures and desirable mechanical properties while eliminating energy-intensive operations [1, 3]. The resulting products exhibit mechanical and metallurgical properties comparable to wrought products. The increasing utilization of sintered metal products is attributed to their ease of working and luxurious surface finish, leading to cost reductions in subsequent finishing processes such as grinding and buffing [4, 5]. Many researchers explore the impact of various factors such as friction and adhesion, both of which are influenced by the applied pressure during the manufacturing process [6, 7]. Deformation of sintered metal is different at high speed as compared to at slow speed due to different flow stress of sintered metal [10, 11, 12]. The impact of speed is of great importance in the forging of sintered metal [13, 14]. Over the years, researchers have tried to quantify dynamic effects of

forging in sintered metal by different mathematical modelling methods, either by the equilibrium method, the upper bound method, or the lower bound method.

The study investigates the theoretical modelling of bulging in sintered preforms on free surfaces and die loads, employing the upper bound method approach. The research examines the effects of various factors such as the degree of bulging, initial relative density, and height reduction on total energy dissipation and die loads, as well as the dissipation of energy in different components. Despite the complexity of the relationships involved, the interplay between these factors forms the cornerstone of the study. A critical analysis is conducted on the influence of die velocity and other deformation characteristics on die loads and energy dissipation, particularly focusing on frictional energy dissipation. It is found that friction energy dissipation plays a predominant role, especially at high forging speeds. While numerous models have been proposed to understand various aspects of sinter-forging problems, there has been a lack of systematic investigation into bulging during high-speed sinter-forging processes. Hence, this paper aims to bridge this gap by employing an energy method analysis using a bulging velocity field to determine energy dissipation and die loads under axial symmetry conditions. The study explores the relationship between frictional energy dissipation, die loads, and other variable calculations. The results are critically discussed to highlight the interactions between various parameters involved in the forging process, and graphical representations are provided for clarity. The degree of bulging developed during forging is shown to depend on factors such as dry and lubricated conditions and the initial density of the disc. Different lubrication conditions can result in varied shapes of bulging, with dry friction leading to more significant barrelling. The impact of lubricant viscosity on bulging is noted, although it requires further study. Developing an additive theory involving the bulging coefficient was challenging to maintain consistency with cases without bulging.

This comprehensive approach will give understanding of bulging during sinter-forging processes, along with the analysis of energy dissipation and die loads, and provide valuable insights for researchers and practitioners in the field, offering a holistic view of the complex interplay of factors involved in high-speed sinter-forging operations. Overall, the paper aims to contribute practical insights for designing software needed for high-speed sinter-forging processes.

2. ENERGY DISSIPATIONS

2.1 Internal Energy Dissipation

$$W_i = \sqrt{\frac{2}{3}}\pi\lambda U b^2(1+\beta)\sqrt{1+\frac{1}{2}\left(\frac{1-2\eta}{1+\eta}\right)^2}$$

Internal energy dissipation has linear proportionality with U.

2.2 Shear Frictional Energy

$$W_f = \int_0^b \tau(|U_r|_{z=0} + |U_r|_{z=h}).2\pi r dr$$

$W_{\mathrm{f}} = \frac{2\pi U(1-2\eta)\mu p_{av} b^3}{(1+\eta)h}\left[\frac{1}{3} + x\left\{\frac{1}{3}\left(1-\frac{r_m}{nb}\right)+\frac{1}{4n}\right\}\right](1+\beta)$; consider $p = p_{av} = \frac{P}{\pi b^2}$

Shear frictional energy also has linear proportionality with speed.

2.3 Inertial Energy Dissipation

$$W_{\mathrm{a}} = \int_0^b \int_0^h \rho_{\mathrm{p}}(a_r U_r + a_z U_z) 2\pi r \, \mathrm{d}r \, \mathrm{d}z$$

$$a_r = \left(\frac{(1-2\eta)}{2(1+\eta)}\frac{r}{h}\right)\left[\frac{(1-2\eta)}{2(1+\eta)}\frac{U^2}{h}(1+\beta) + \dot{U}\right](1+\beta)$$

$$a_z = \frac{z}{h}\left(\frac{U^2}{h}(1+\beta) - \dot{U}\right)(1+\beta)$$

$$W_a = 2\pi\rho_p b^2(1+\beta)\left[U^3(1+\beta)\left\{\frac{b}{3h^2}\left(\frac{(1-2\eta)}{2(1+\eta)}\right)^3 + \frac{1}{6}\right\} + \mathrm{U}\dot{U}\left\{\frac{b^3}{3h}\left(\frac{(1-2\eta)}{2(1+\eta)}\right)^2 - \frac{h}{6}\right\}\right]$$

3. FORGING LOAD, P

$$P = \frac{\sqrt{\frac{2}{3}}\pi\lambda b^2\sqrt{1+\frac{1}{2}\left(\frac{1-2\eta}{1+\eta}\right)^2} + 2\pi\rho_p b^2\left[U^2(1+\beta)\left\{\frac{b}{3h^2}\left(\frac{(1-2\eta)}{2(1+\eta)}\right)^3+\frac{1}{6}\right\} + \dot{U}\left\{\frac{b^3}{3h}\left(\frac{(1-2\eta)}{2(1+\eta)}\right)^2 - \frac{h}{6}\right\}\right]}{1 - \frac{2(1-2\eta)\mu b}{(1+\eta)h}\left(\frac{1}{3} + x\left\{\frac{1}{3}\left(1-\frac{r_m}{nb}\right)+\frac{1}{4n}\right\}\right)}$$

$$p_{av} = \frac{\sqrt{\frac{2}{3}}\lambda\sqrt{1+\frac{1}{2}\left(\frac{1-2\eta}{1+\eta}\right)^2} + 2\rho_p\left[U^2(1+\beta)\left\{\frac{b}{3h^2}\left(\frac{(1-2\eta)}{2(1+\eta)}\right)^3+\frac{1}{6}\right\} + \dot{U}\left\{\frac{b^3}{3h}\left(\frac{(1-2\eta)}{2(1+\eta)}\right)^2 - \frac{h}{6}\right\}\right]}{1 - \frac{2(1-2\eta)\mu b}{(1+\eta)h}\left(\frac{1}{3} + x\left\{\frac{1}{3}\left(1-\frac{r_m}{nb}\right)+\frac{1}{4n}\right\}\right)}$$

$$\frac{p_{av}}{\lambda} = \frac{\sqrt{\frac{2}{3}}\sqrt{1+\frac{1}{2}\left(\frac{1-2\eta}{1+\eta}\right)^2} + \frac{2\rho_p}{\lambda}\left[U^2(1+\beta)\left\{\frac{b}{3h^2}\left(\frac{(1-2\eta)}{2(1+\eta)}\right)^3+\frac{1}{6}\right\} + \dot{U}\left\{\frac{b^3}{3h}\left(\frac{(1-2\eta)}{2(1+\eta)}\right)^2 - \frac{h}{6}\right\}\right]}{1 - \frac{2(1-2\eta)\mu b}{(1+\eta)h}\left(\frac{1}{3} + x\left\{\frac{1}{3}\left(1-\frac{r_m}{nb}\right)+\frac{1}{4n}\right\}\right)}$$

4. RESULTS AND DISCUSSION

Some extra energy dissipation is required in bulging during plastic deformation by the platen at the free surface. The magnitude of extra energy dissipation also depends on the degree of bulging. The root cause of bulging is the interfacial friction between the platen and the workpiece interface. The degree of bulging depends on bulging coefficient β. Here we are considering only constant bulging, because friction and bulging are too complicated behaviours. Bulging and friction depend on various factors, such as the coefficient of friction, die velocity, etc. The speed parameter exerts a substantial impact on the bulging of sintered preforms, yet there has been relatively limited research conducted on this crucial aspect. The influence of speed on bulging preform during the forging process is a critical factor that can significantly affect various deformation characteristics and final product properties. More in-depth research on the effect of speed will enhance our understanding of its implications in

sintered preform forging. Exploring this aspect further could lead to valuable insights for optimizing the forging process, improving efficiency, and achieving desired material properties in the final products. The friction energy dissipation fraction increase by due to high-speed forging result in heating on the workpiece die interaction surface which results in increase temperature at surface and temperature increment inside the workpiece also but it is less than at surface temperature. Friction is an evil in metal forming; it causes extra energy dissipation and bulging, resulting in product geometry. For the preforms with higher relative density ρ, a greater load P is needed for deformation.

$\lambda = 1070.7\text{kg/cm}^2$, $\mu = 0.3$, $b = 1.1\text{cm}$, $h = 1\text{cm}$, $n = 2.0$, $\rho_p = 0.0027\text{kg/cm}^3$, $\dot{U} = 0$,x =0.3.

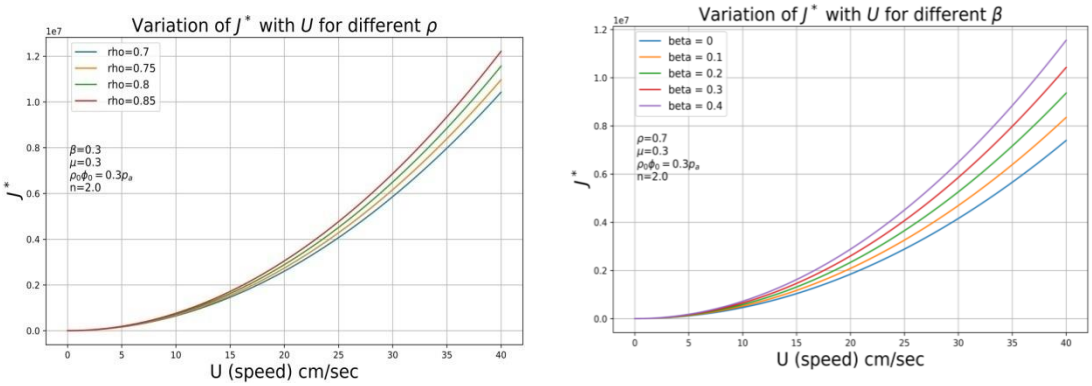

(a) (b)

Figure 1: Variation of J^* with U under different scenarios, $\dot{U}$ =1cm/sec^2

By figure 1 total energy dissipation during the forging of sintered preforms increases rapidly after a die speed of 5cm/sec, varying with bulging coefficient and initial relative density.

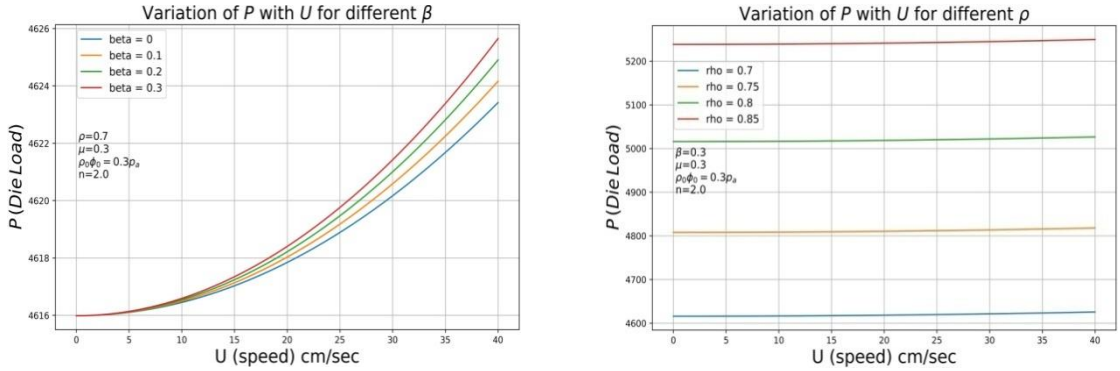

(a) (b)

Figure 2: Variation of P with U under different scenarios.

By figure 2, the required die load, P, during the forging of sintered preforms increases rapidly after a die speed of 5 cm/sec for different bulging coefficients. High initial relative density workpieces require more die load for plastic deformation of the sintered disk during forging.

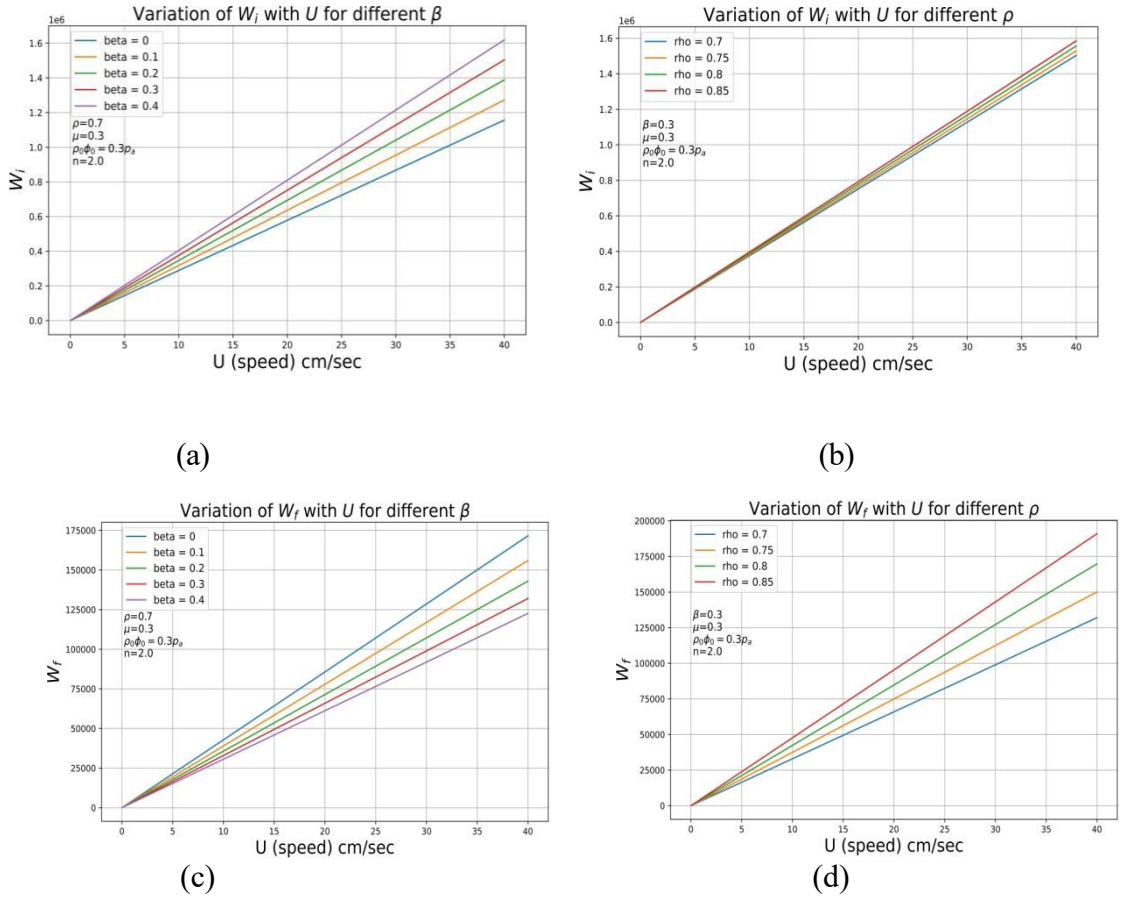

Figure 3: Variation of W_i, W_f with U for different ρ and β

By figure 3, total energy dissipation during the forging of sintered preforms increases rapidly after a die speed of 5 cm/sec, varying with bulging coefficient and initial relative density. A higher bulging coefficient and initial relative density require greater energy for plastic deformation of the disk during forging.

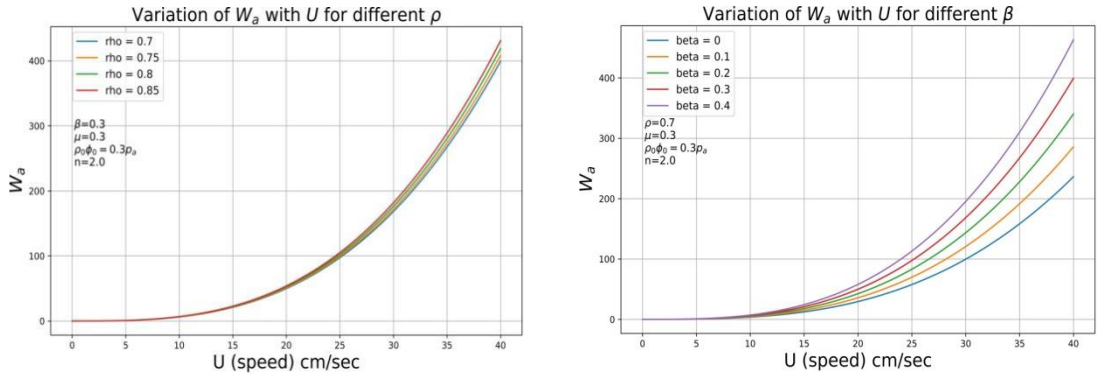

Figure 4: Variation of W_a with U for different ρ and β

By figure 4, total dissipation due to inertial energy during the forging of sintered preform increases rapidly after a die speed of 5 cm/sec, varying with bulging coefficient and initial relative density. A higher bulging coefficient and initial relative density require greater inertial energy for plastic deformation of the disk during forging.

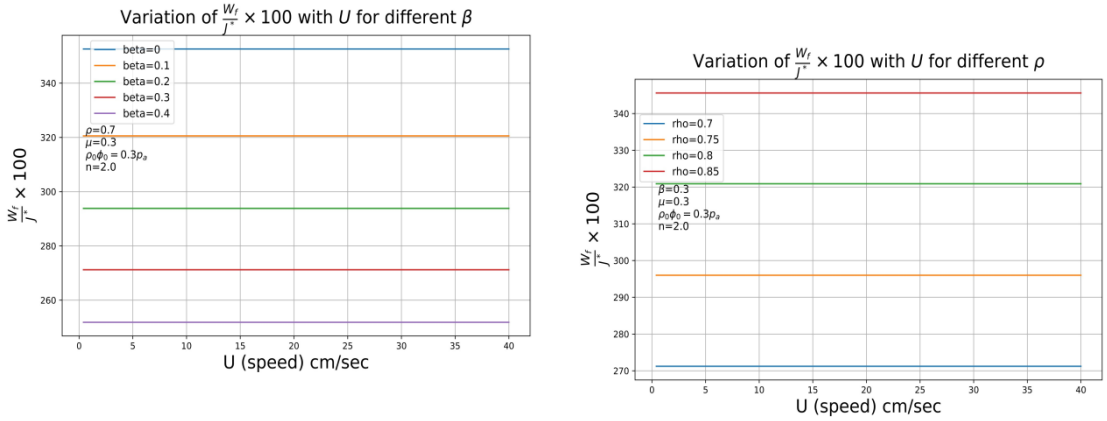

(a) (b)

Figure 5: Variation of W_f with U for different ρ and β

By figure 5, the relative shear frictional energy to total energy dissipation during forging of sintered preform increases with die speed, bulging coefficient and initial relative density. Higher bulging coefficient and initial relative density necessitate greater frictional energy dissipation for plastic deformation during forging.

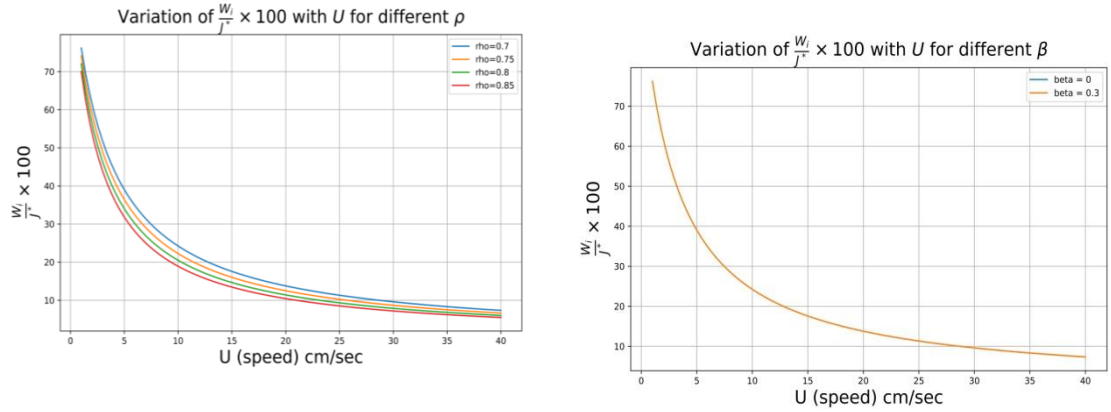

(a) (b)

Figure 6: Variation of $\frac{W_i}{J^*_{J*}}$ with U for different ρ and β.

By figure 6, the relative fractional internal energy dissipation decreases with an increase in bulging coefficient and relative density. There exists an intricate relationship between fractional internal energy dissipation and fractional frictional energy dissipation, where one increases while the other decreases accordingly. At high die velocities, most of the energy is dissipated as frictional energy in the form of heat, leading to bulging of the profile. Therefore,

it is advisable to limit the forging operation to a certain velocity to achieve the desired finished product.

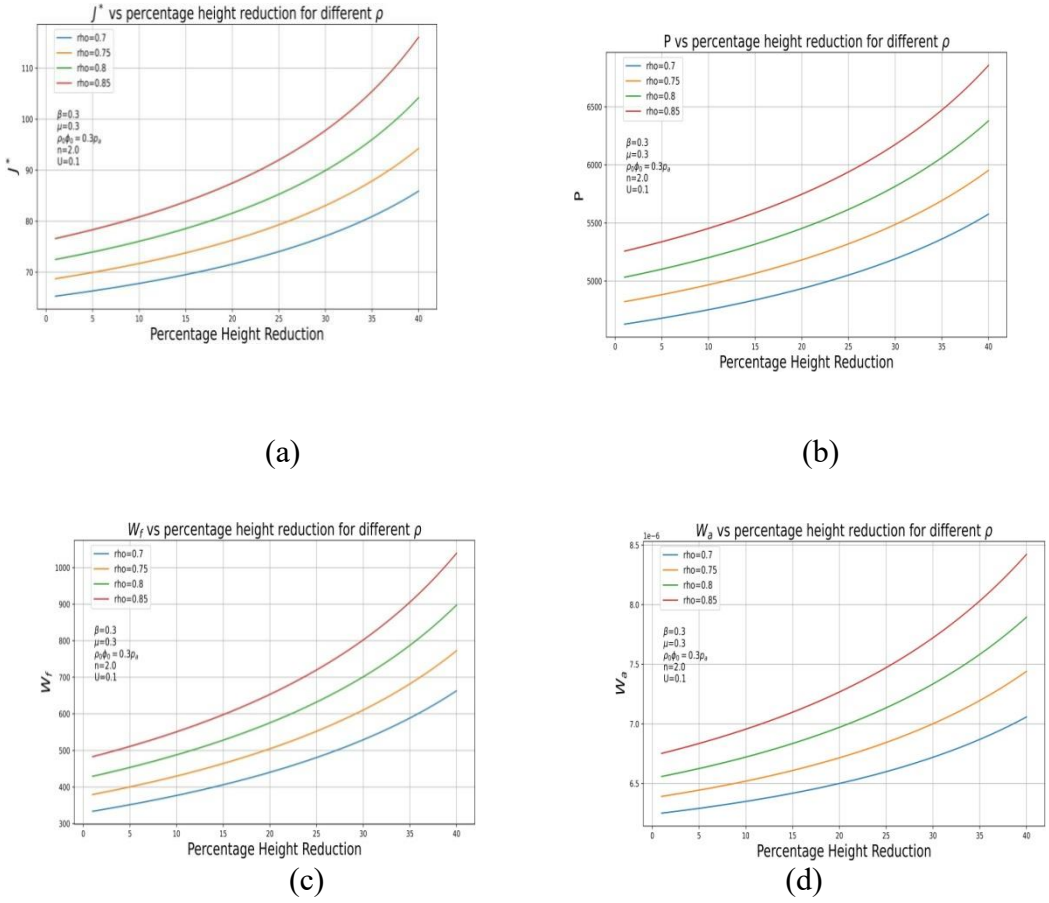

Figure 7: Variation of J^*, P, W_f, W_a with % height reduction for different ρ

By figure 7, there is a sharp increase in total energy dissipation, die load, frictional energy dissipation, and inertial energy dissipation with a reduction in height after a 5% height reduction. The majority of the energy is dissipated in the form of heat, which can be mitigated to some extent by using lubricants. However, it cannot be neglected, as ideal conditions are rarely achievable. The heat is produced on the surface as well the temperature of the workpiece also increases.

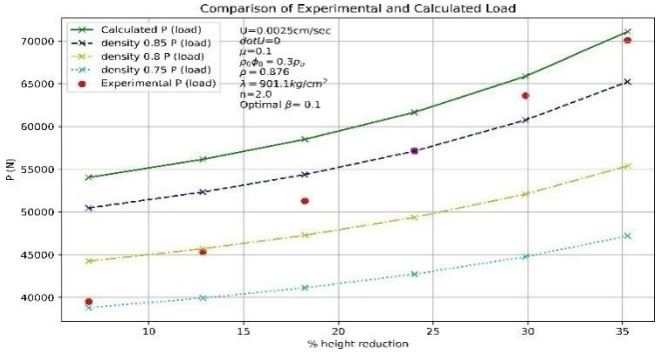

Figure 8

As upper method always predicts more load than the required, we find the optimal value of β = 0.1. As the upper method always predicts more load than is required, we find the optimal value of $\beta = 0.1$. Figure 8 illustrates the convergence between the experimental and theoretical curves for the bulging profile; the observation is consistent [19]. The close alignment between experimental and theoretical results for bulging energy dissipation theory underscores the potential applicability of our model within industrial contexts.

This convergence suggests that our model holds promise for accurately estimating die load across diverse operational parameters, including speed variations, initial relative density, bulging discrepancies, alterations in preform dimensions, and variations in the degree of adhesion during height reduction processes.

5. CONCLUSION

The forging process of sintered preforms involves significant energy dissipation, influenced by factors such as die speed, bulging coefficient, initial relative density, and height reduction during forging.

- High die speeds lead to increased frictional energy dissipation, resulting in surface heating and bulging.
- Additionally, there's a sharp increase in energy dissipation, die load, and frictional energy with a 5% reduction in height, primarily dissipating as heat on the preform surface. While lubricants can mitigate this, the resulting temperature rise affects the workpiece surface and, to some extent, its interior.
- Total energy dissipation, die load, and frictional energy increase notably after a 5 cm/sec die speed, especially with higher bulging coefficients and initial relative densities. Inertial energy dissipation also rises rapidly under these conditions.

The relationship between fractional internal energy dissipation and fractional frictional energy dissipation to total energy dissipation is intricate, with fractional internal energy dissipation decreasing while the other fractional frictional energy dissipation component increases with bulging coefficient and relative density. At high die velocities, most energy dissipates as frictional heat, necessitating control of forging velocity to achieve desired product outcomes.

The implications of our model for industrial processes are significant, as it offers the capability to precisely estimate die load under varying conditions. Such predictive capabilities are crucial for optimizing manufacturing processes, enhancing efficiency, and ensuring product quality.

6. CONFLICT OF INTEREST

On behalf of all authors, the corresponding author states that there is no conflict of interest.

Acknowledgments:

Navdeep's work is supported by the Council of Scientific and Industrial Research (CSIR), Govt. of India (Award no. 09/1256(15849)/2022-EMR-1). Dr. Parveen Kumar expresses his gratitude for the financial support from the Department of Science & Technology, New Delhi, India for Purse (SR/PURSE/2022/126).

REFERENCES

1. Cull G. W., "Mechanical and metallurgical properties of powder forgings", 1970.
2. Singh S., Jha A. K., "Sintered preforms adds better value to aerospace components", Journal of Aerospace Engineering, I. E. (I), 82, (2001), 1-6.
3. Jones P. K., "The technical and economic advantage of powder forged products", Powder Metallurgy, Vol. 13, Issue 26, (1970), 114-129.
4. Cost savings win the day for PM parts, Metal Powder Report, Vol. 56 (7-8), (2001), 10-14.
5. Jha A. K. and Kumar S., "Compatibility of sintered materials during cold forging", International Journal of Materials and Product Technology, Vol. 9, Issue 4-6, (1994), 281-299. 10.1504/IJMPT.1994.036423
6. Tabata T., Masaki S. and Abe Y., "Analysis of Forging P/M Preforms" Journal of the Japan Society for Technology of Plasticity, 18, (1977), 373.
7. Tabata T., Masaki S. and Hosokawa K., "A Compression Test to Determine the Coefficient of Friction in Forging P/M Preforms", International Journal of Powder Metallurgy Powder Technology, 16, (1980), 149.
8. Jha A. K. and Kumar S., "Analysis of Axisymmetric Cold Processing of Metal Powder Preforms", Journal of the Institution of Engineers (India), 65, (1985), 169.
9. Jha A. K., Kumar S., "Investigations into the high-speed forging of sintered copper powder strips", Journal of Materials Processing Technology,71(3), (1997), 394-401. 10.1016/S0924-0136(97)00104-0
10. Jha A. K., Kumar S., "Dynamic effects during a high-speed sinter-forging process", International Journal of Machine Tools and Manufacture, Vol. 36, Issue 10, (1996), 1109-1122, ISSN 0890-6955. 10.1016/0890-6955(95)00122-0
11. Agrawal M., Jha A. K., Kumar S., "High-speed forging of hollow metal powder preforms", Inst. Engrs. (I) J., 80 (1999),8.
12. Singh Saranjit, Jha A.K., "Analysis of dynamic effects during high-speed forging of sintered preforms", Journal of Materials Processing Technology, Volume 112, Issue 1, 2001,Pages 53-62, ISSN 0924-0136. 10.1016/S0924-0136(00)00898-0
13. Singh Saranjit & Jha A. K. & Kumar Suhas. "Dynamic effects during sinter forging of axi-symmetric hollow disc preforms", International Journal of Machine Tools and Manufacture, Vol. 47, Issue 7-8,(2007),1101-1113. 10.1016/J.IJMACHTOOLS.2006.09.023
14. Singh S., Jha A. K., "An energy analysis during forging of sintered truncated conical preform at high-speed", Tamkang J. of Science and Engineering,7,(2004), 227-236. http://jase.tku.edu.tw/articles/jase-200412-7-4-05
15. Kumar Parveen, Ranjan R. K., Kumar Rajive, "Mathematical modelling of forging of sintered preform: Comparative study of open and closed die", International Journal of Pure and Applied Mathematics, Vol. 82, Issue 2, (2012), 179-188.

https://www.ijpam.eu/contents/2013-82-2/2/2.pdf

16. Kumar Parveen, Ranjan R. K., Kumar Rajive, **"**Mechanics of deformation during open die forging of sintered preform: Comparative study by equilibrium and upper bound methods", ARPN Journal of Engineering and Applied Sciences, 6(6), (2011)83–93.

    https://arpnjournals.com/jeas/research_papers/rp_2011/jeas_0611_515.pdf

17. Kumar Parveen, Ranjan R. K., Kumar Rajive, "Investigations of an axisymmetric compound flow behavior of sintered preform: An upper bound approach", International Journal of Pure and Applied Mathematics, Vol. 81, Issue 5, (2012), 671-691.

    https://www.ijpam.eu/contents/2012-81-5/2/2.pdf

18. Avitzur B., "Metal Forming Processes and Analysis", McGraw Hill, New York, 1968.
19. Jain Shrikant, Ranjan R. K. and Kumar Surender, "Fracturing and Deformation Characteristics of Aluminium Preform during Cold Forging at Low Strain Rates". Int. J. of Scientific Engineering and Technology, 4(3) (2015),182-186. 10.17950/ijset/v4s3/314

NOMENCLATURE

h	instantaneous thickness of the work piece
n	constant quantity much greater than unity
p	pressure at the die-work piece interface
r, θ,z	cylindrical co-ordinates
x, y, z	Cartesian co-ordinates
P	die load
U	die velocity
$\dot{U}$	acceleration
U_i	displacement rate field
ΔV	magnitude of the relative velocity
b	radius of the disc
ε	strain
ε_{ij}	corresponding strain rate tensor field
η	constant and a function of relative density ρ
λ	flow stress of the sintered material
μ	co-efficient of friction
ρ_p	initial density of the sintered preform
a_i	associated acceleration field

σ_0 yield stress of the non-work hardening matrix metal

τ shear stress

ϕ_0 specific cohesion of the contact surface

W_i internal energy dissipation

W_f frictional shear energy

W_a inertial force energy

$$\xi(\%) = \left(|p/\lambda|_{\text{withdynamiceffect}} - |p/\lambda|_{\text{withoutdynamiceffect}}\right)/|p/\lambda|_{\text{withdynamiceffect}}$$

APPENDIX

Velocity Field, Strain Rates

$$U_r = \frac{(1-2\eta)}{2(1+\eta)}\frac{U}{h}r(1+\beta),\ U_z = -z\frac{U}{h}(1+\beta),\ U_\theta = 0$$

satisfy the compatibility equation $\frac{\partial U_r}{\partial r} + \frac{(1-2\eta)}{2(1+\eta)}\frac{\partial U_z}{\partial z} = 0$

Chosen the kinetically admissible velocity field which satisfies the boundary conditions, $|U_z|_{z=0} = 0$ and $|U_z|_{z=h} = U$.

The strain rates are:

$$\dot{\varepsilon}_{rr} = \frac{\partial U_r}{\partial r} = \frac{(1-2\eta)}{2(1+\eta)}\frac{U}{h}(1+\beta)\ ;\ \dot{\varepsilon}_{\theta\theta} = \frac{U_r}{r} = \frac{(1-2\eta)}{2(1+\eta)}\frac{U}{h}(1+\beta)\ ;\ \dot{\varepsilon}_{zz} = \frac{\partial U_z}{\partial z} = -\frac{U}{h}(1+\beta)$$

$$\dot{\varepsilon}_{r\theta} = \frac{1}{2}\left(\frac{\partial U_\theta}{\partial r} - \frac{\partial U_\theta}{\partial r} + \frac{1}{r}\frac{\partial U_r}{\partial \theta}\right) = 0\ ;\ \dot{\varepsilon}_{rz} = \frac{1}{2}\left(\frac{\partial U_r}{\partial z} + \frac{\partial U_z}{\partial r}\right) = 0\ ;\ \dot{\varepsilon}_{\theta z} = \frac{1}{2}\left(\frac{\partial U_z}{\partial \theta} + \frac{\partial U_\theta}{\partial z}\right) = 0$$

$$\dot{\varepsilon}_{rr} = \dot{\varepsilon}_{\theta\theta}$$

Upper Bound Limit Analysis

$$J^* = \frac{2\sigma_0}{\sqrt{3}}\int_v \sqrt{\frac{1}{2}\dot{\varepsilon}_{ij}\dot{\varepsilon}_{ij}}\,\mathrm{d}v + \int_s \tau|\Delta V|\mathrm{d}s + \int_v \rho_p a_i U_i\,\mathrm{d}v\ ;\quad J^* = PU = W_i + W_f + W_a$$

$$W_i = \frac{2\sigma_0}{\sqrt{3}}\int_v \sqrt{\frac{1}{2}\dot{\varepsilon}_{ij}\dot{\varepsilon}_{ij}}\,\mathrm{d}v\ ;\ W_f = \int_s \tau|\Delta v|\mathrm{d}s\ ;\ W_a = \int_v \rho_p a_i U_i\,\mathrm{d}v$$

Where $a_r = U_r\frac{\partial U_r}{\partial r} + U_z\frac{\partial U_r}{\partial z} + \frac{\partial U_r}{\partial t},\ a_z = U_z\frac{\partial U_z}{\partial z} + \frac{\partial U_z}{\partial t}$